The GCM Response to Current Parameterizations of Nonorographic Gravity Wave Drag

(McLandress and Scinocca, 2005)

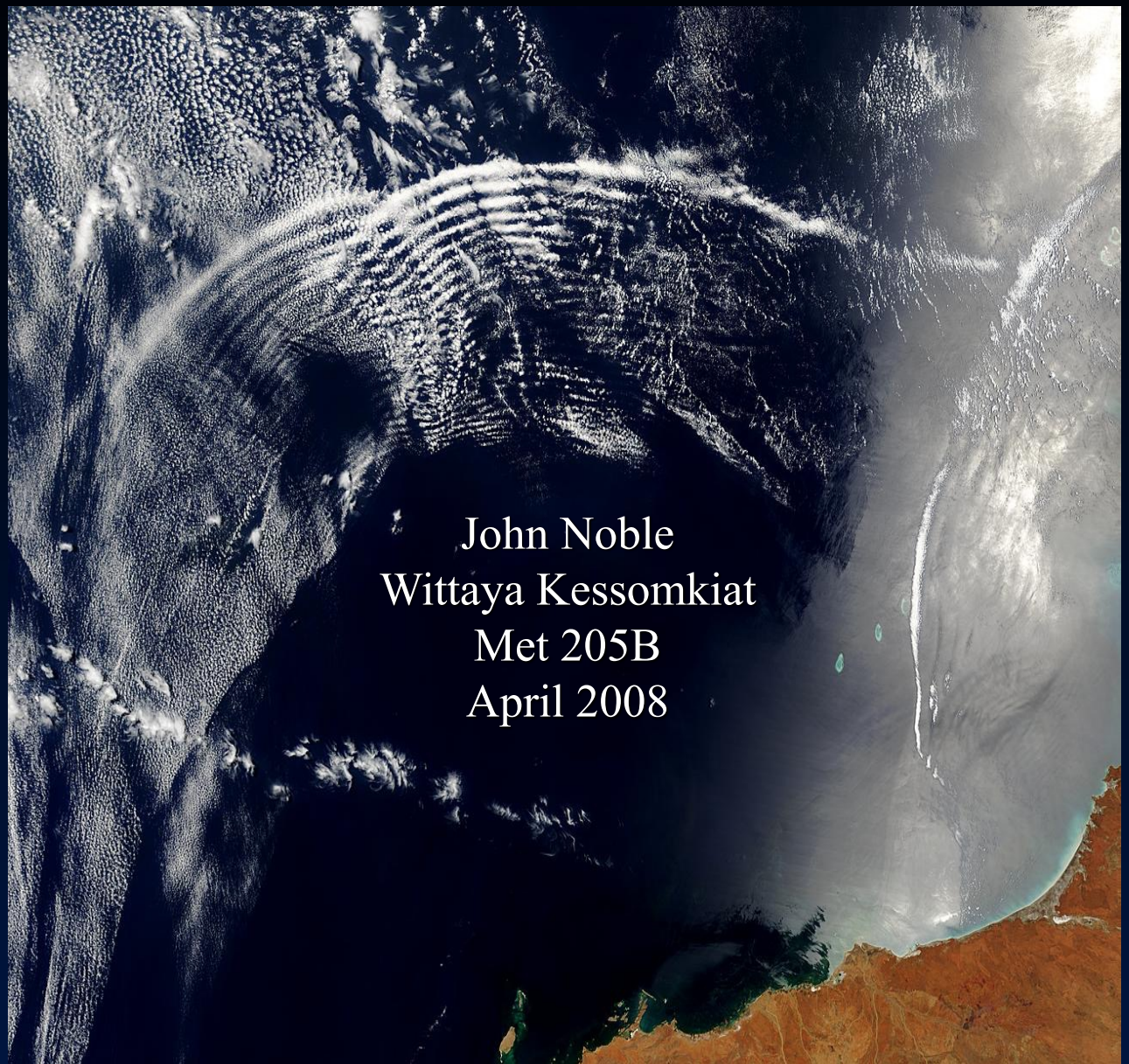

John Noble
Wittaya Kessomkiat
Met 205B
April 2008

Objective

- To compare and document the GCM response that is due to differences in the dissipation mechanisms themselves.

- To understand the source of the differences in the GCM response.

McLandress, C., and J. F. Scinocca, 2005: The GCM Response to Current Parameterizations of Nonorographic Gravity Wave Drag. *J. Atmos. Sci*., **62**, 2394–2413

Introduction

- Spectral GWD parameterizations
  - Bring about zonal-mean zonal wind reversals in the mesosphere.
  - Alleviate the winter stratosphere cold bias in the SH.
  - Produce an earlier breakdown of the SH winter vortex.
  - Help drive realistic stratospheric quasi-biennial and mesospheric semiannual oscillations.

- Dissipation mechanisms
  - Understanding to sensitivity of the GCM response to the choice of dissipation mechanism.
  - Examining the dissipation mechanisms employed in the 3 nonorographic GWD parameterizations that are currently used in middle atmosphere GCMs.

Generalized spectral parameterization

Achieved by coding the dissipation mechanisms into the same parameterization schemes

a) Launch spectrum and conservative propagation

- Restrict the linear wave dynamics to be hydrostatic
- Ignore the effects of rotation

$$m^2 = \frac{k^2 N^2}{\hat{\omega}^2}, \text{where } \hat{\omega} = \omega - kU$$

Assume function form and total momentum flux is independent of time and geographic location

$$\hat{E}_o\left(m, \hat{\omega}, \phi\right) = B\left(\frac{m}{m_*}\right) \frac{N_o^2 \hat{\omega}^{-p}}{1 + \left(\frac{m}{m_*}\right)^4}$$

A schematic of the momentum flux density at the launch level is illustrated in Fig. 1a.

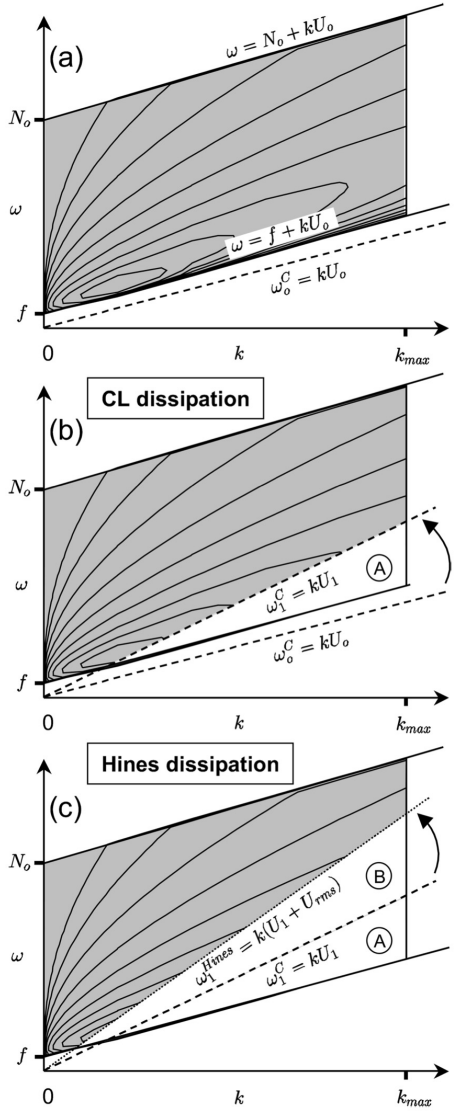

FIG. 1. Schematic of momentum flux density ρF as a function of wavenumber k and ground-based frequency ω for a single horizontal azimuth. The shaded regions indicate nonzero values of ρF. (a) Momentum flux density ρF at launch level 0, where the dashed line ω_o^C corresponds to pairs of k and ω for which the launch level is a critical level; (b) ρF at level 1 due to critical-level dissipation that occurs during the propagation of the spectrum from the level below when $U_1 > U_o$, an amount of momentum flux equal to the integral of ρF over the region A is deposited to the flow; (c) ρF at level 1 due to critical-level dissipation and Hines dissipation. The application of the latter results in additional momentum deposition that is equal to the integral of ρF over the region B. See text for details.

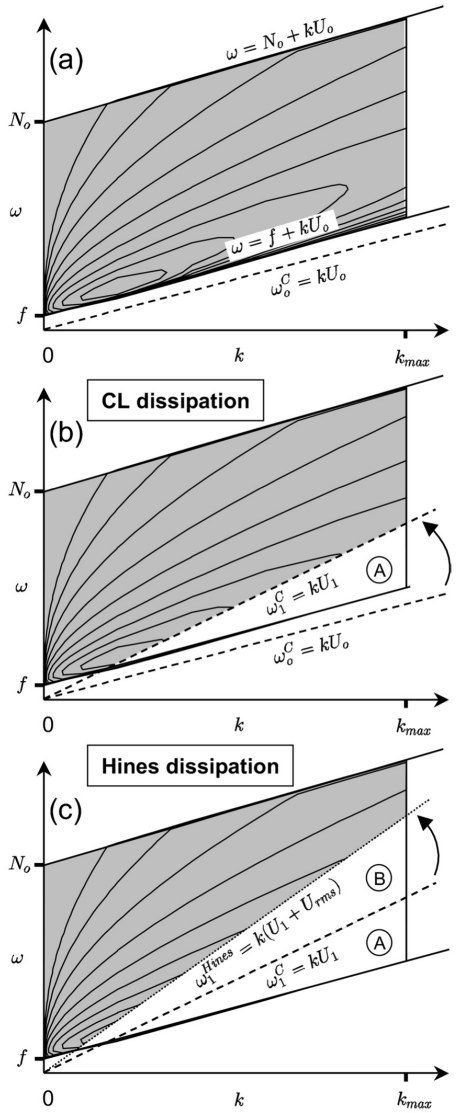

FIG. 1. Schematic of momentum flux density ρF as a function of wavenumber k and ground-based frequency ω for a single horizontal azimuth. The shaded regions indicate nonzero values of ρF. (a) Momentum flux density ρF at launch level 0, where the dashed line ω_o^C corresponds to pairs of k and ω for which the launch level is a critical level; (b) ρF at level 1 due to critical-level dissipation that occurs during the propagation of the spectrum from the level below when $U_1 > U_o$, an amount of momentum flux equal to the integral of ρF over the region A is deposited to the flow; (c) ρF at level 1 due to critical-level dissipation and Hines dissipation. The application of the latter results in additional momentum deposition that is equal to the integral of ρF over the region B. See text for details.

Generalized spectral parameterization

b) Critical-level and nonlinear dissipation

1. Critical-level dissipation (Fig. 1b)

- Wavenumber and frequencies (A region) have undergone critical-level filtering b/w these 2 levels.
- Wavenumber and frequencies (shade) survive critical-level dissipation and are free to conservatively propagate upward to the next vertical level.

2. Nonlinear dissipation

a) Hines dissipation (Fig. 1c)

- Causes critical-level filtering to extend to additional wavenumbers and frequencies
- A+B region yield the amount of momentum deposited by the wave field to the background flow
- Shaded areas are free to consrvatively propagate upward to the next vertical level

Generalized spectral parameterization

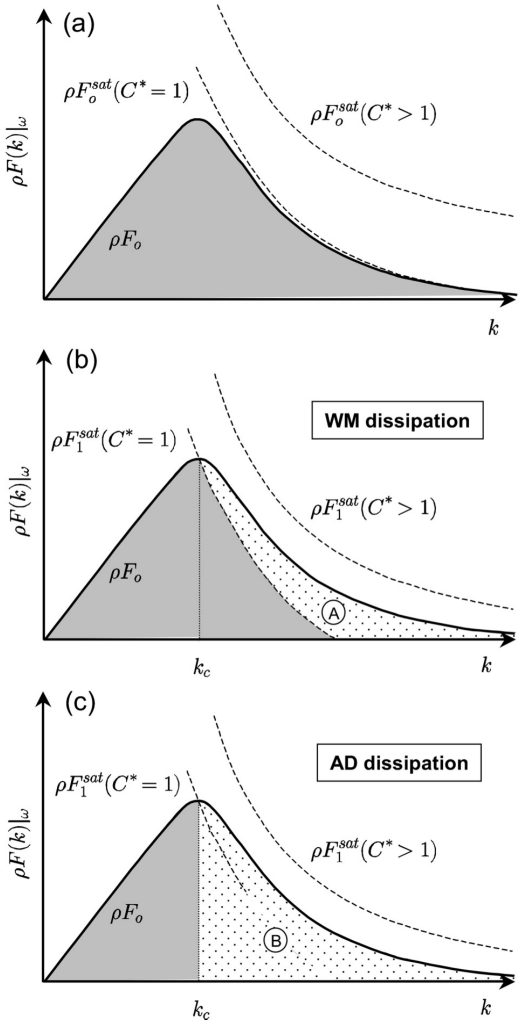

FIG. 2. Schematic of momentum flux density ρF as a function of wavenumber k at constant frequency ω for the case of $U = 0$ at all levels. The dashed curves represent the saturated spectrum used to define WM and AD dissipation for two values of C^* (see text). (a) At launch level 0; (b) WM dissipation at level 1: At $k = k_c$ the saturation curve for $C^* = 1$ has intersected ρF. For $k > k_c$, ρF is set equal to the value of the saturated spectrum, resulting in a momentum deposition that is equal to the integral of ρF over the stippled region A. (c) AD dissipation at level 1: the WM criterion is used to determine all wavenumbers and frequencies that become unstable between the launch level and level 1. Setting ρF to zero for these spectral elements results in an amount of momentum deposition that is equal to the integral of ρF over the stippled region B.

2. Nonlinear dissipation (cont.)

b) Warner and McIntyre (WM) dissipation

- Assume the nonlinear dissipation may be modeled by limiting the wave energy density at large vertical wavenumbers to the observed m^{-3} functional form (Fig. 2a).

$$\rho F^{\mathrm{sat}}\left(k,\omega,\phi\right) = C^* D \frac{\omega^{3/2}}{k^3}$$

$$\rho F_o\left(k,\omega,\phi\right) = D_o \frac{\omega^{3/2} k}{k^4 + \left(m_* \omega \Big/ N_o\right)^4}$$

- Fig. 2b shows how the saturation bound induces dissipation in the wave field at a higher elevation.

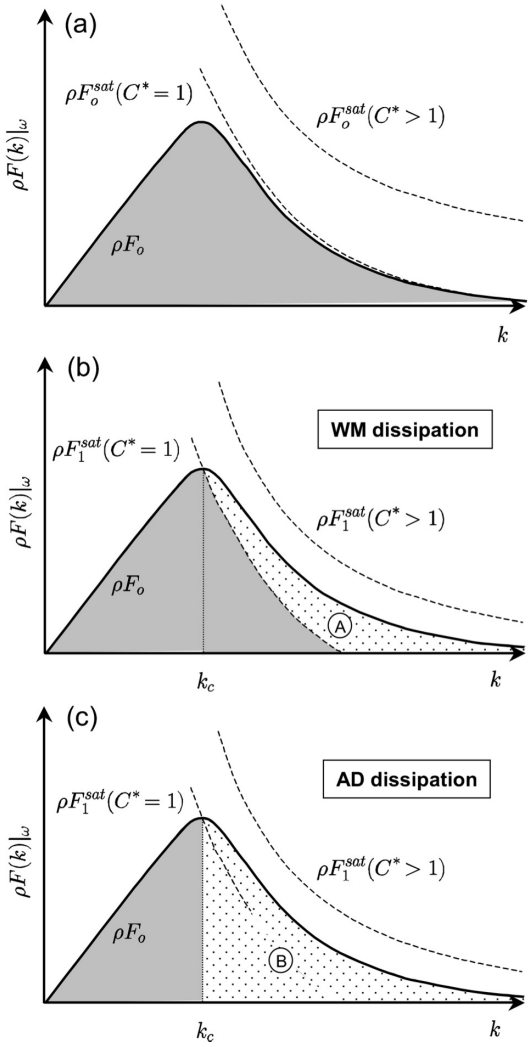

FIG. 2. Schematic of momentum flux density ρF as a function of wavenumber k at constant frequency ω for the case of $U = 0$ at all levels. The dashed curves represent the saturated spectrum used to define WM and AD dissipation for two values of C^* (see text). (a) At launch level 0; (b) WM dissipation at level 1: At $k = k_c$ the saturation curve for $C^* = 1$ has intersected ρF. For $k > k_c$, ρF is set equal to the value of the saturated spectrum, resulting in a momentum deposition that is equal to the integral of ρF over the stippled region A. (c) AD dissipation at level 1: the WM criterion is used to determine all wavenumbers and frequencies that become unstable between the launch level and level 1. Setting ρF to zero for these spectral elements results in an amount of momentum deposition that is equal to the integral of ρF over the stippled region B.

Generalized spectral parameterization

2. Nonlinear dissipation (cont.)

c) Alexander and Dunkerton (AD) dissipation

- Nonlinear dissipation may be equally well modeled by depositing all of the launch momentum flux of a spectral element at the altitude of the initial onset of instability.
- All wavenumbers to the right of kc initially satisfy the WM dissipation criterion b/w the launch level and level 1.
- Consequently, the momentum flux density of each spectral element to the right of k_c is set to zero and an amount of momentum flux equal to area B is deposited to the flow in this azimuth. (Fig. 2c)

Response to dissipation mechanisms

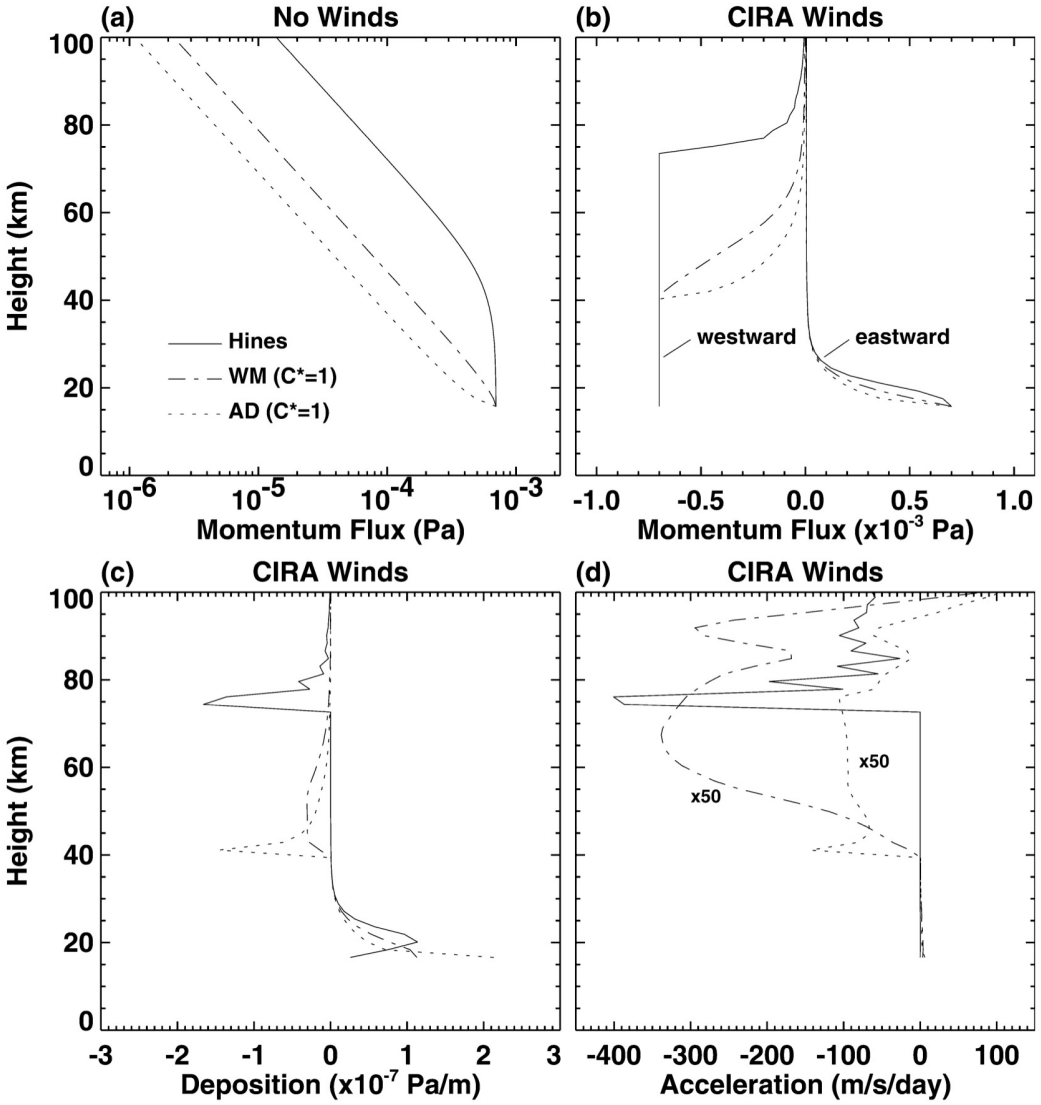

FIG. 3. Offline calculations using Hines, WM, and AD dissipation. (a) Momentum flux in a single azimuth for calculations without mean winds (using a constant buoyancy frequency of 0.02 s^{-1}). (b) Eastward and westward components of the momentum flux for calculations using the CIRA wind and buoyancy frequency for Jun at 50°S, and the corresponding (c) momentum deposition and (d) acceleration. The launch level is located near 16 km. For WM and AD dissipation a value of $C^* = 1$ is used and the acceleration has been multiplied by a factor of 50.

The comparison of the GCM response to the 3 nonlinear dissipation mechanisms.

a) Offline calculations

- No mean-wind shear because critical-level dissipation associated with the background wind is absent
- more rapid decrease AD>WM>Hines (Fig. 3a)
- The effect of critical-level filtering by the background eastward wind in now seen by rapid decarease with height of the eastward component of the momentum flux (Fig. 3b)

Response to dissipation mechanisms

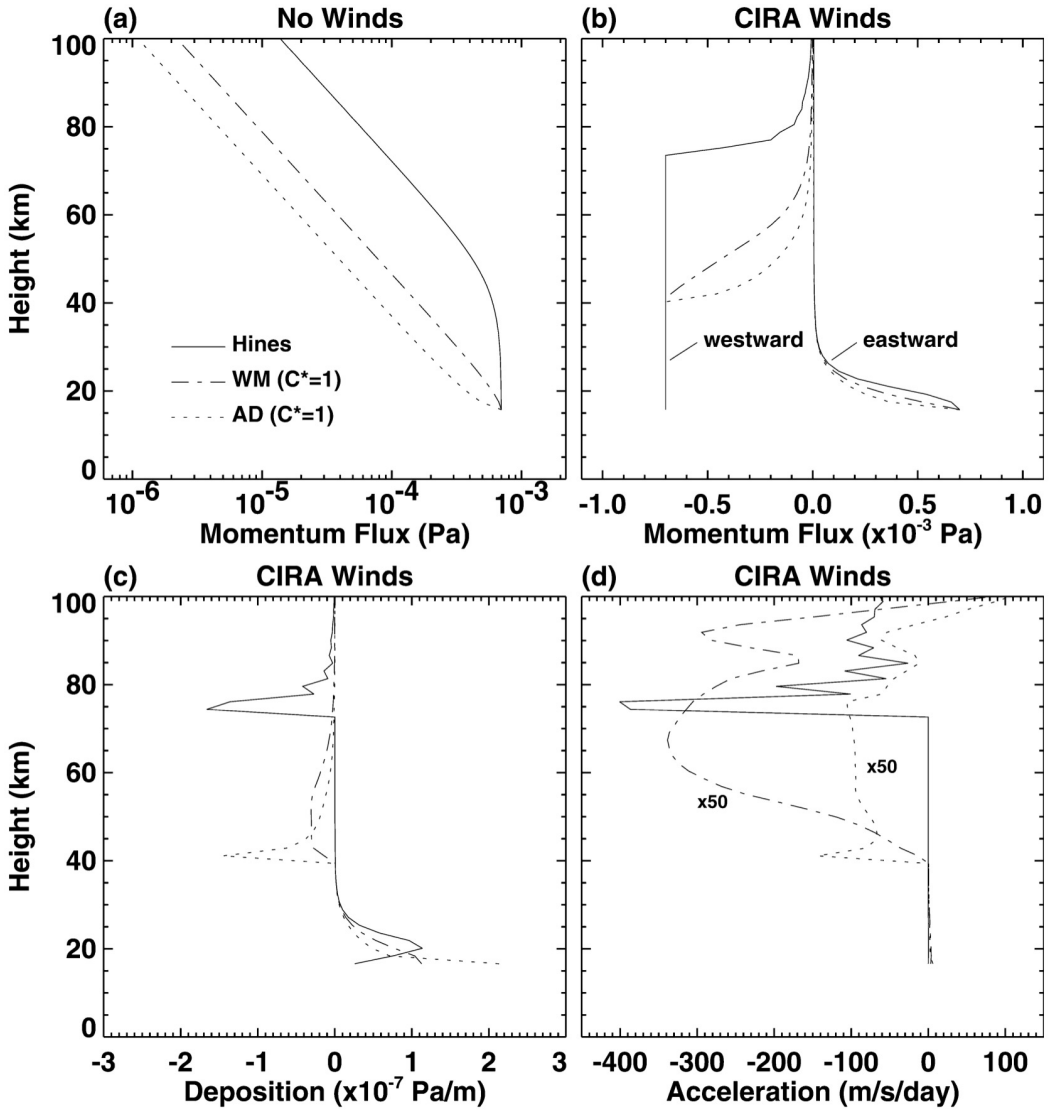

FIG. 3. Offline calculations using Hines, WM, and AD dissipation. (a) Momentum flux in a single azimuth for calculations without mean winds (using a constant buoyancy frequency of 0.02 s^{-1}). (b) Eastward and westward components of the momentum flux for calculations using the CIRA wind and buoyancy frequency for Jun at 50°S, and the corresponding (c) momentum deposition and (d) acceleration. The launch level is located near 16 km. For WM and AD dissipation a value of $C^* = 1$ is used and the acceleration has been multiplied by a factor of 50.

a) Offline calculations (cont.)

- The height at which the westward component of the fluxes starts decreasing are greater than in the no-wind case (Fig. 3a).
- Substantial difference in the peak elevation and vertical structure of the momentum deposition for each of the dissipation mechanisms (Fig. 3c)
- The acceleration displays the expected enhancement in the mesosphere for the Hines and WM dissipation mechanism (Fig. 3d)

Response to dissipation mechanisms

b) GCM simulations

Use GCM extending from surface to ~100 km with T32 horizontal resolution and 65 vertical levels

- Computational constraints much coarser than a).
- Focus on the solstice seasons when the zonal winds are strongest in the extratropics.
- The zonal-mean zonal winds and momentum deposition for JJA and DJF are shown in Figures 5 and 6 at the surface and at 100 hPa.
- Most striking in the summer mesosphere with westerlies speeds nearly 100 m s^{-1} and near 100 hPa (Fig. 6).
- Fig. 7 indicates that overall, the application of nonorographic GWD produces winds at 52.6º S and 52.6º N that are weaker than simulations without nonorographic GWD (no-GWD case).
- The stronger eastward that result when the waves are launched near 100 hPa (*e.g.,* top panels of Fig. 6) arise because there is no tropospheric filtering. This behavior occurs for all three dissipation mechanisms as can be seen from the corresponding vertical profiles of momentum deposition shown in Fig. 8.

Response to dissipation mechanisms

b) GCM simulations (cont.)

- Comparing the relative magnitudes of the Hines momentum deposition in the summer and winter mesosphere, for example, we see that it is largest in winter when the waves are launched near the ground, but largest in summer when the waves are launched near the tropopause.

- Momentum from the offline calculations is deposited much higher in the extratropical middle atmosphere for Hines.

- AD winds are most similar to the no-GWD case (Fig. 7).

- The energy dissipation arising from the application of the Hines scheme is more realistic than that produced by WM.

Response to dissipation mechanisms

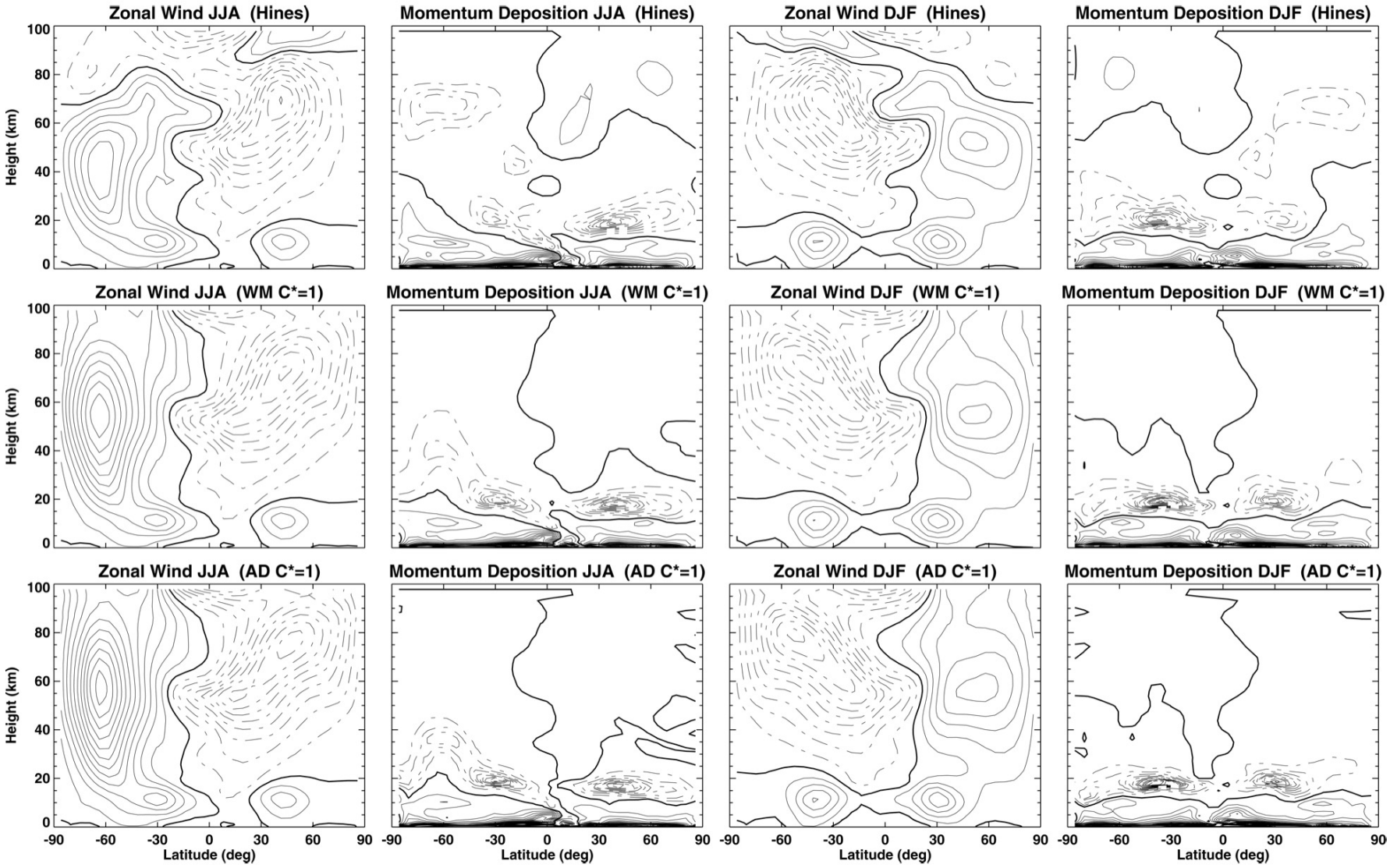

FIG. 5. Zonal-mean zonal wind and momentum deposition for simulations using (top) Hines, (middle) WM, and (bottom) AD dissipation for (two left columns) JJA and (two right columns) DJF. The launch level is located near the surface. A value of $C^* = 1$ is used for WM and AD dissipation. Contour intervals of 10 m s^{-1} and 2×10^{-8} Pa m^{-1} are used. Easterlies and negative values of deposition are dashed; the zero lines are thick.

Response to dissipation mechanisms

Ignoring for the time being the momentum deposition, inspection of these figures reveals that the wind response to Hines dissipation exhibits by far the largest changes in the mesosphere. This is most striking in the summer mesosphere, where the westerlies attain speeds of nearly 100 m s^{-1} in the case where the launch height is located near 100 hPa (Fig. 6).

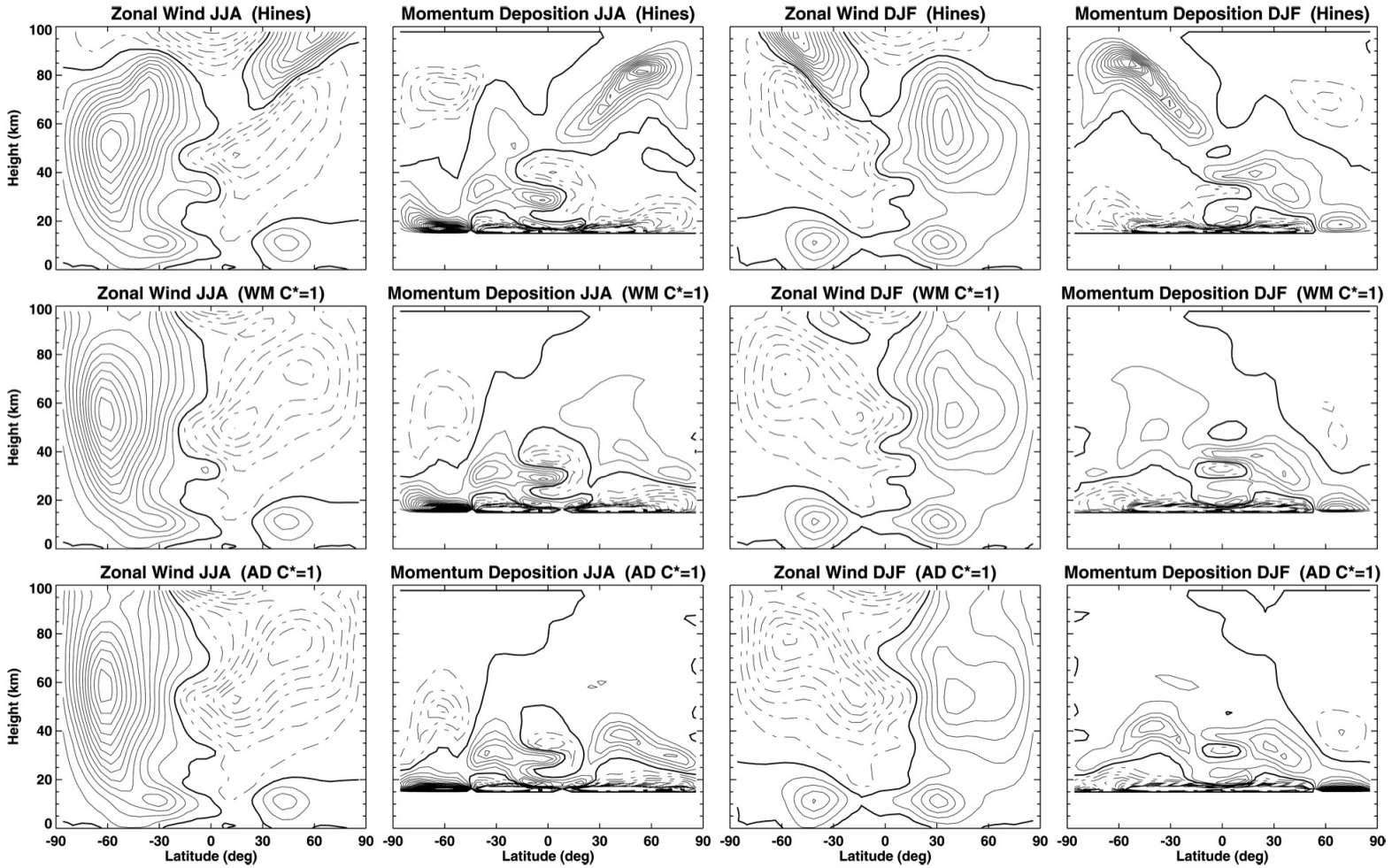

FIG. 6. Same as Fig. 5 but for a launch level near 100 hPa (~16 km). A contour interval of 1×10^{-8} Pa m^{-1} is used for momentum deposition.

Response to dissipation mechanisms

Fig. 7 indicates that overall, the application of nonorographic GWD produces winds at 52.6º S and 52.6º N that are weaker than the no-GWD case.

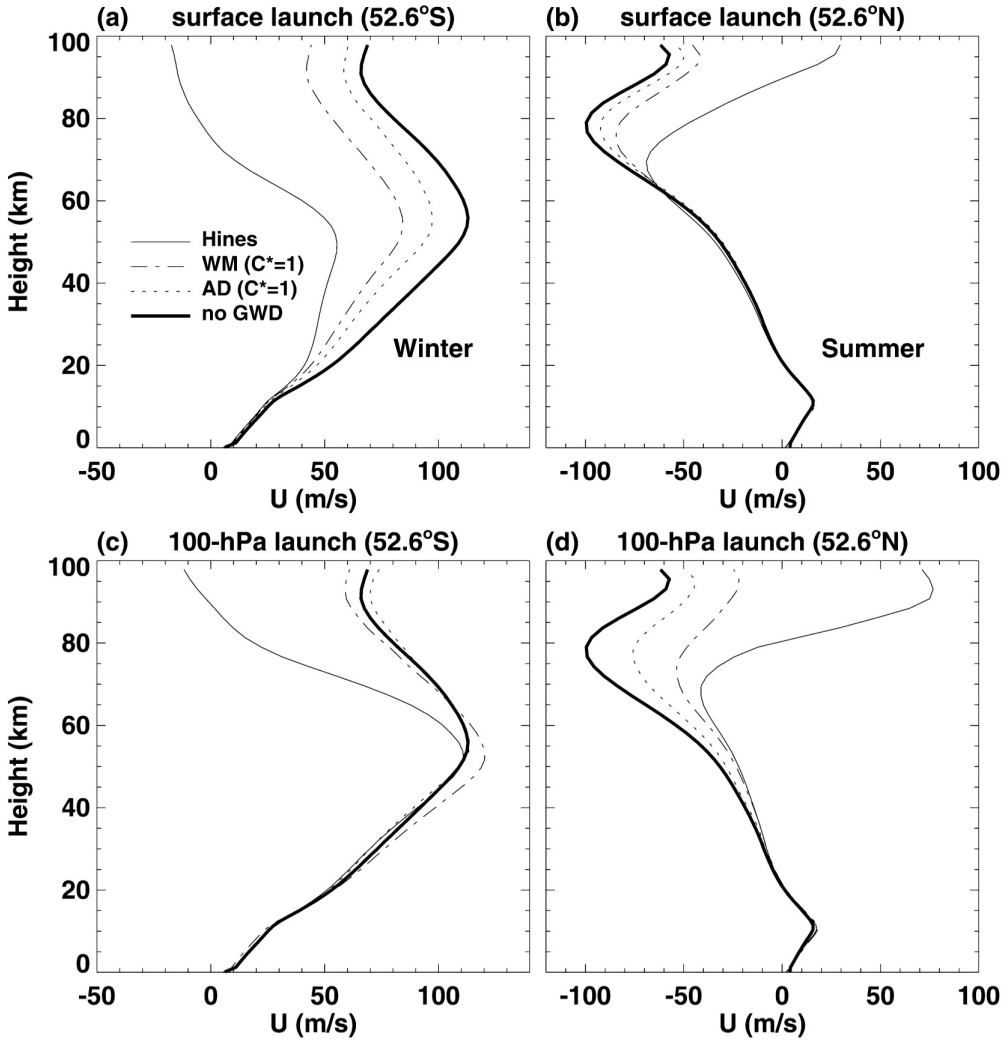

FIG. 7. Zonal-mean zonal wind profiles for simulations using Hines, WM, and AD dissipation for JJA for the launch level near the surface: (a) 52.6°S and (b) 52.6°N, and for the launch level near 100 hPa (~16 km): (c) 52.6°S and (d) 52.6°N. The corresponding contour plots are shown in Figs. 5 and 6. The thick solid line is for a 5-yr simulation without nonorographic GWD.

Response to dissipation mechanisms

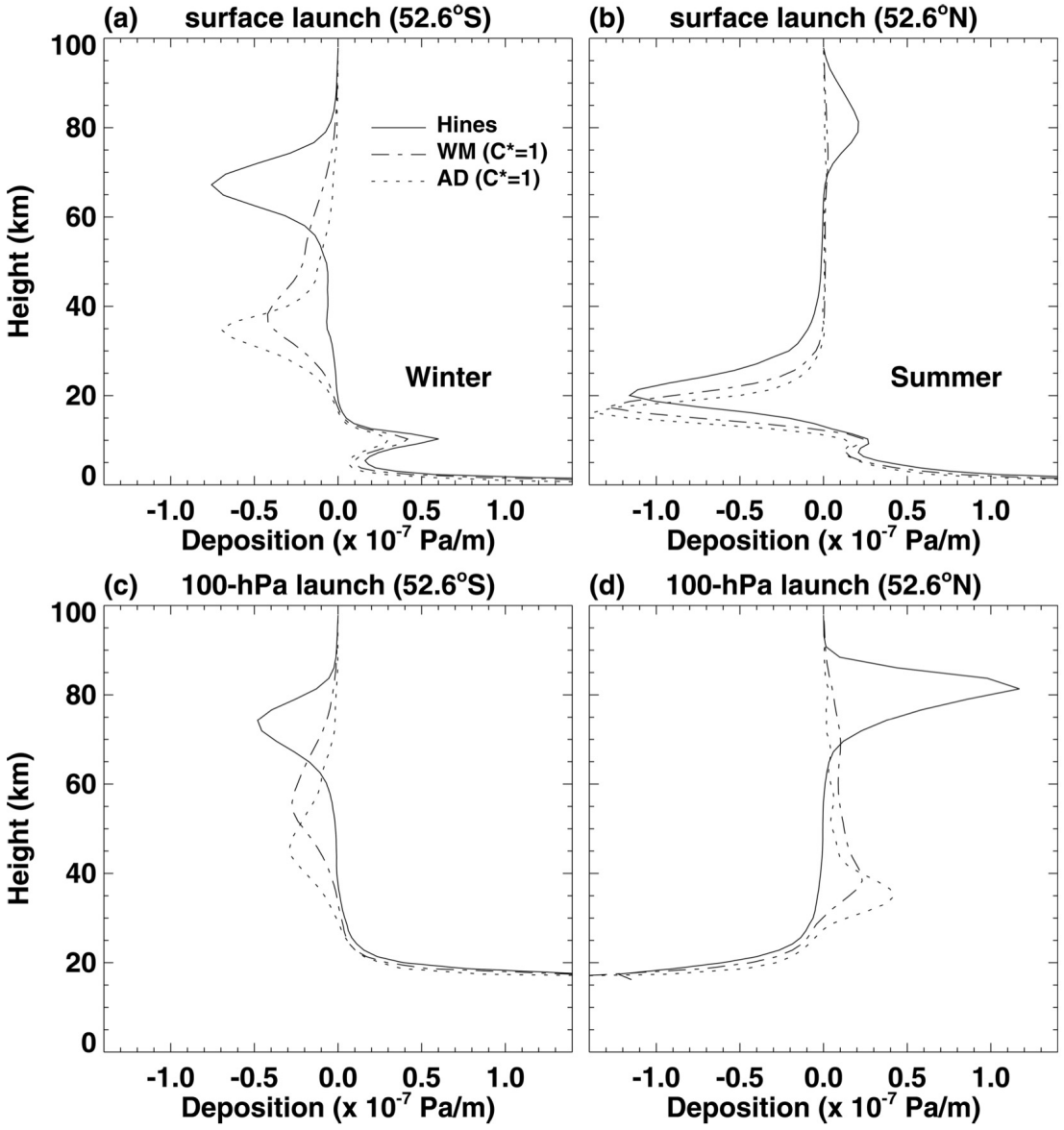

FIG. 8. Zonal-mean momentum deposition profiles for simulations using Hines, WM, and AD dissipation for JJA for the launch level near the surface: (a) 52.6°S and (b) 52.6°N, and for the launch level near 100 hPa (~16 km): (c) 52.6°S and (d) 52.6°N. The corresponding contour plots are shown in Figs. 5 and 6.

Sensitivity experiments

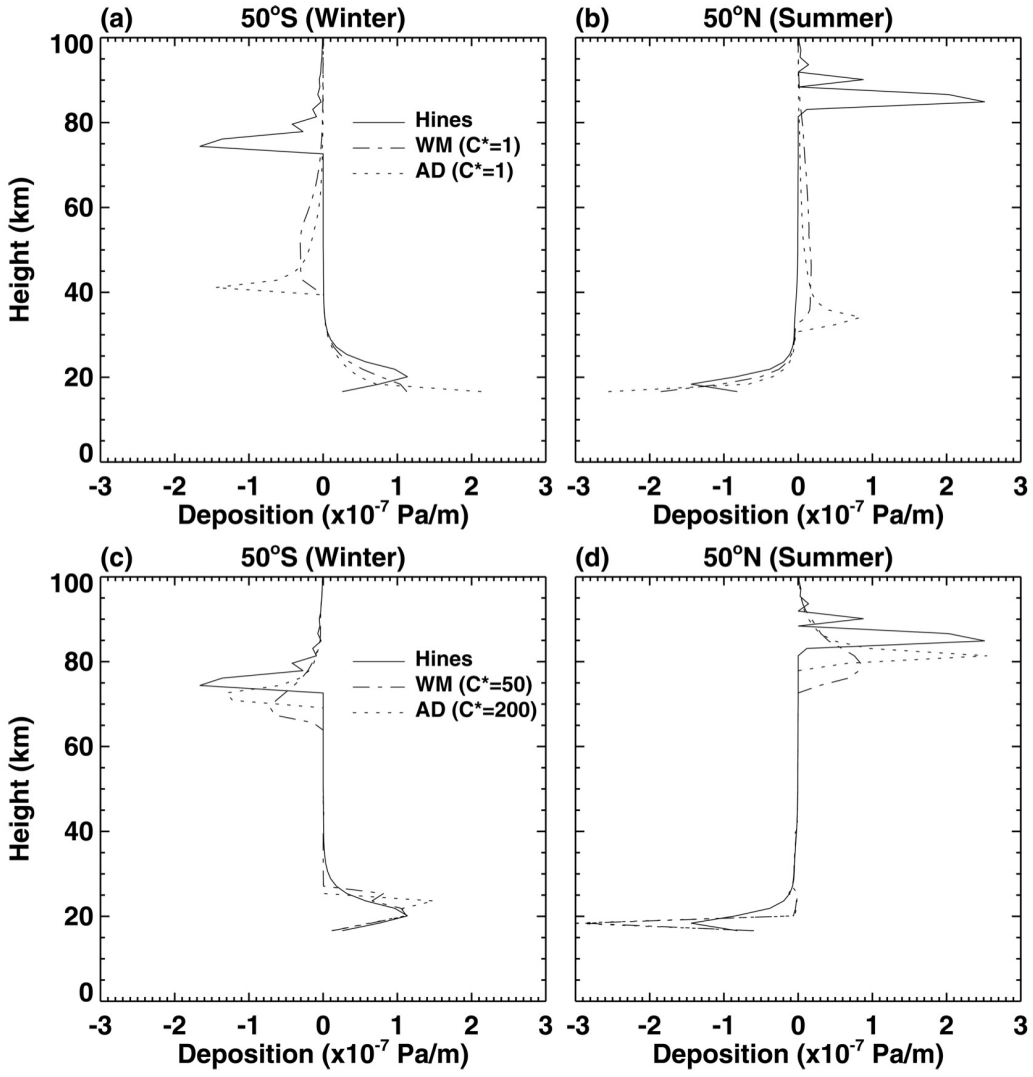

FIG. 9. Momentum deposition profiles computed offline using CIRA winds and temperatures for Jun. (a) Hines, WM ($C^* = 1$), and AD ($C^* = 1$) at 50°S; (b) same as (a) but at 50°N; (c) Hines, WM ($C^* = 50$), and AD ($C^* = 200$) at 50°S; and (d) same as (c) but at 50°N.

a) Offline calculations

- Comparison of the top and bottom rows of Fig. 9 show that the new settings for C^* reduce most of the systematic difference in the elevation of momentum deposition between the schemes.
- Have some control over the height of momentum deposition for both AD & MM dissipation but no control over its vertical structure

b) GCM simulations

- All 3 schemes show the strong reversal in the summer mesosphere and the slight equatorward tilt of the winter mesosphere jet similar for winter as well (Fig. 10, ignore the bottom row and 2 right columns)

Sensitivity experiments

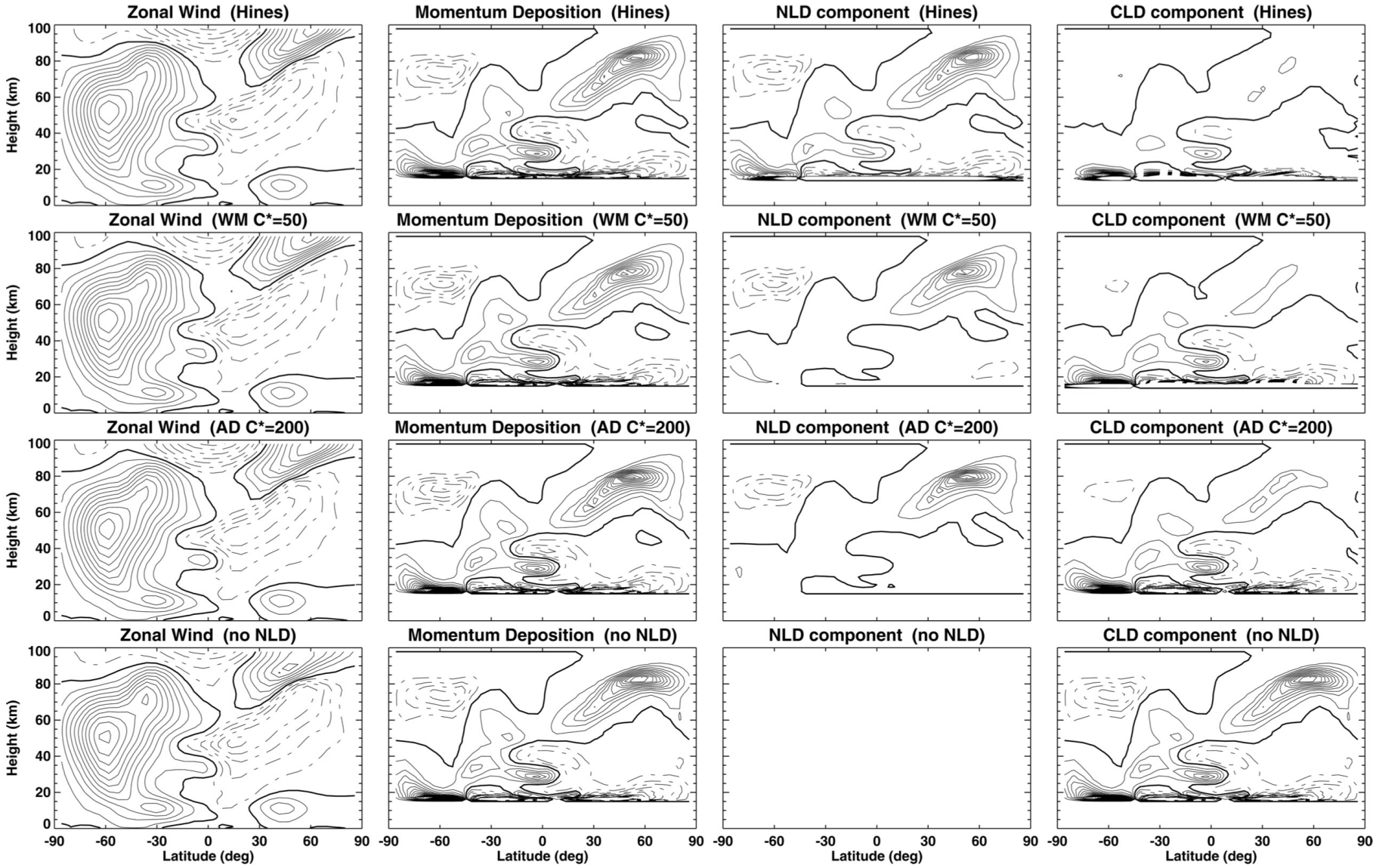

FIG. 10. (first column) JJA zonal-mean zonal wind, (second column) momentum deposition, (third column) components of momentum deposition due to nonlinear dissipation, and (fourth column) critical-level dissipation. Top row is for a simulation using Hines, second row using WM with $C^* = 50$, third row using AD with $C^* = 200$, and bottom row without nonlinear dissipation. The launch level is near 100 hPa (~16 km). Contour intervals are the same as in Fig. 6.

Sensitivity experiments

b) GCM simulations (cont.)

- The 2nd column of Fig. 10 shows similarity of winds from 3 simulations because the latitude-height distribution is essentially indistinguishable.

- From the offline calculation, it appears that feedback processes in the GCM reduce differences in the nonlinear dissipation mechanisms.

- The zonal winds and momentum deposition are virtually indistinguishable from other three (bottom row of Fig. 10 with only critical-level dissipation) [without nonlinear dissipation].

- Inspection of this decomposition for each of the Hines, WM ($C^* = 50$), and AD ($C^* = 200$) simulations reveals that nearly all of the momentum deposition above 50 km is dominated by nonlinear dissipation and not by CL dissipation.

- It is only when the nonlinear dissipation is turned off that CL dissipation effectively takes its place above 50 km (row 4, final column of Fig. 10).

Sensitivity experiments

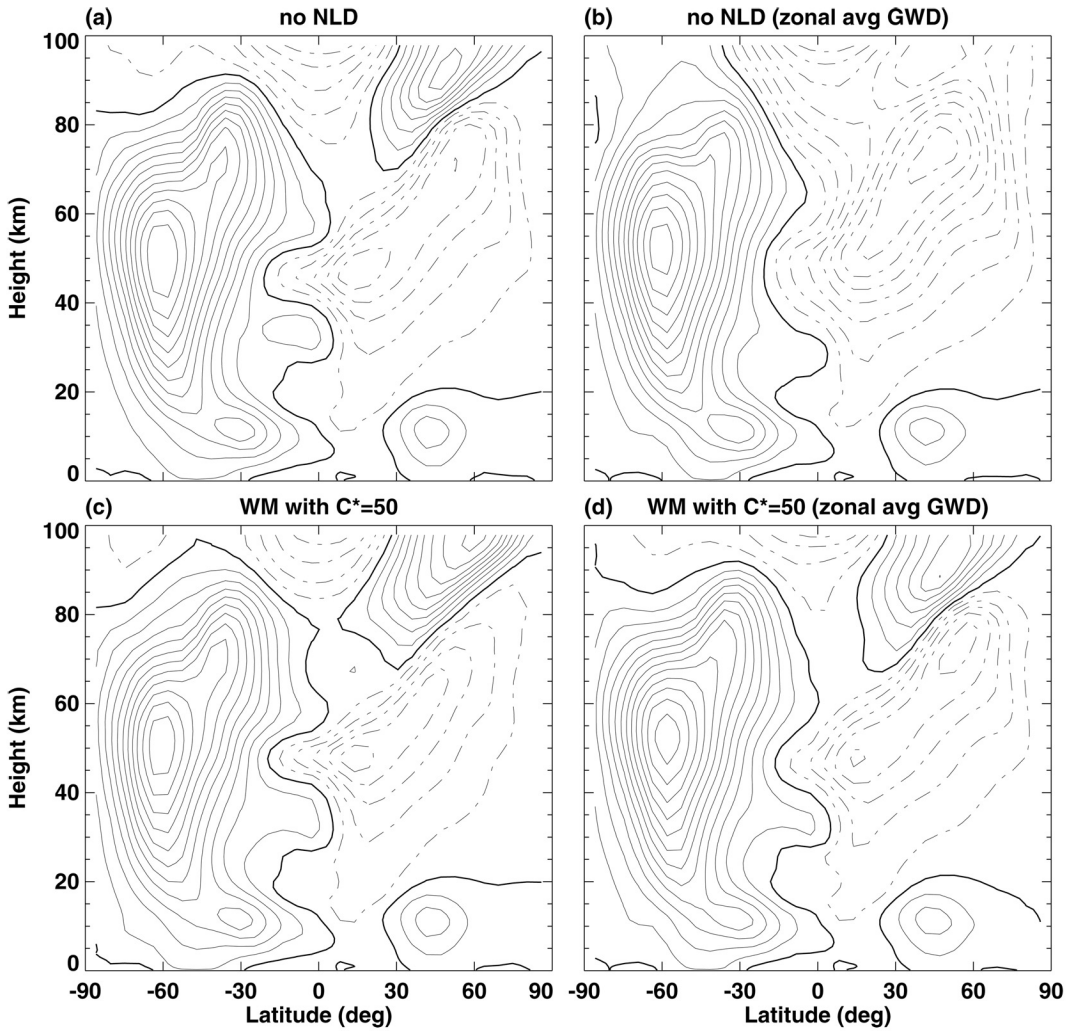

FIG. 11. Zonal-mean zonal wind for a single JJA for simulations without nonlinear dissipation (i.e., using only CL dissipation in the GSP): (a) the third year of the 5-yr ensemble shown in Fig. 10 and (b) a seasonal integration for the same third year JJA, initialized in Apr, in which the GWD is computed using the zonal mean, rather than local, winds, and temperatures. (c), (d) Same as (a) and (b) but for simulations using WM dissipation with $C^* = 50$. A contour interval of 10 m s^{-1} is employed; easterlies are dashed.

b) GCM simulations (cont.)

- The expectation is that the zonal averaging will eliminate critical levels caused by longitudinal disturbances and prevent the onset of the summertime mesosphere wind reversal (Fig. 11).
- This behavior is clearly borne out in Fig. 11b.
- With the inclusion of nonlinear dissipation, the GCM response is relatively insensitive to longitudinal disturbances (Fig. 11c & 11d)

Summary

- Significant differences between the various nonlinear dissipation mechanisms have little or no impact on the GCM response.

- The GCMs cannot be used in a straightforward manner to validate these dissipation mechanisms.

- Efforts might be better invested in other aspects of the parameterization problem such as the properties of the source spectra which should have more impact on the GCM response than the details of the nonlinear dissipation.